

# Laserspray Ionization, a New Method for Protein Analysis Directly from Tissue at Atmospheric Pressure with Ultrahigh Mass Resolution and Electron Transfer Dissociation\*<sup>§</sup>

Ellen D. Inutan<sup>‡</sup>, Alicia L. Richards<sup>‡</sup>, James Wager-Miller<sup>§</sup>, Ken Mackie<sup>§</sup>, Charles N. McEwen<sup>¶</sup>, and Sarah Trimpin<sup>‡</sup>||

**Laserspray ionization (LSI) mass spectrometry (MS) allows, for the first time, the analysis of proteins directly from tissue using high performance atmospheric pressure ionization mass spectrometers. Several abundant and numerous lower abundant protein ions with molecular masses up to ~20,000 Da were detected as highly charged ions from delipidated mouse brain tissue mounted on a common microscope slide and coated with 2,5-dihydroxyacetophenone as matrix. The ability of LSI to produce multiply charged ions by laser ablation at atmospheric pressure allowed protein analysis at 100,000 mass resolution on an Orbitrap Exactive Fourier transform mass spectrometer. A single acquisition was sufficient to identify the myelin basic protein N-terminal fragment directly from tissue using electron transfer dissociation on a linear trap quadrupole (LTQ) Velos. The high mass resolution and mass accuracy, also obtained with a single acquisition, are useful in determining protein molecular weights and from the electron transfer dissociation data in confirming database-generated sequences. Furthermore, microscopy images of the ablated areas show matrix ablation of ~15  $\mu\text{m}$ -diameter spots in this study. The results suggest that LSI-MS at atmospheric pressure potentially combines speed of analysis and imaging capability common to matrix-assisted laser desorption/ionization and soft ionization, multiple charging, improved fragmentation, and cross-section analysis common to electrospray ionization. *Molecular & Cellular Proteomics* 10: 10.1074/mcp.M110.000760, 1–8, 2011.**

Tissue imaging by mass spectrometry (MS) is proving useful in areas such as detecting tumor margins, determining

sites of high drug uptake, and mapping signaling molecules in brain tissue (1–8). Imaging using secondary ion mass spectrometry is well established but is only marginally useful with intact molecular mass measurements from biological tissue (9–11). Matrix-assisted laser desorption/ionization (MALDI)-MS operating under vacuum conditions has been used for tissue imaging with success, especially for abundant components such as membrane lipids, drug metabolites, and proteins (12–14). Spatial resolution of ~20  $\mu\text{m}$  has been achieved (15), and the MALDI-MS method has been applied in an attempt to shed light on Parkinson disease (16, 17), muscular dystrophy (18), obesity, and cancer (12, 19).

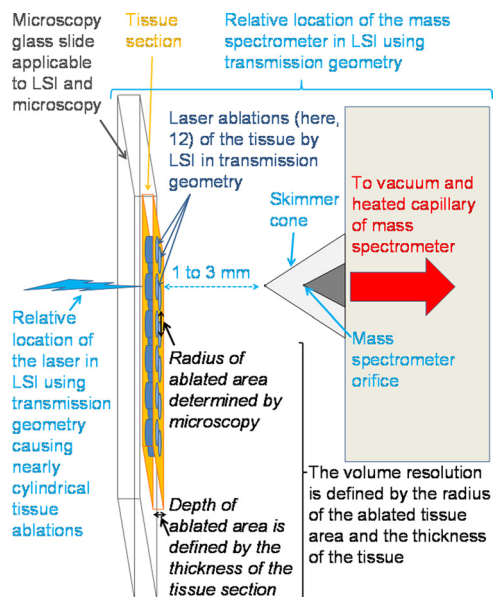
Unfortunately, there are disadvantages in using vacuum-based MS for tissue imaging in relation to analysis of unadulterated tissue. Also, the mass spectrometers used in these studies frequently have much lower mass resolution and mass accuracy than are available with atmospheric pressure ionization (API)<sup>1</sup> instruments and are not as widely available. Because the vacuum ionization methods produce singly charged ions, mass-selected fragmentation methods provide only limited information, especially for proteins. In addition, no advanced fragmentation such as electron transfer dissociation (ETD) (20–22) is available for confident protein confirmation or identification. Atmospheric pressure (AP) MALDI can be coupled to high performance mass spectrometers but suffers from sensitivity issues for tissue imaging where high spatial resolution is desired (23). AP MALDI also primarily produces singly charged ions (24, 25). Thus, mass and cross-section analysis of intact proteins has yet to be accomplished using AP MALDI because of intrinsic mass range limitations of API instruments, which frequently have a mass-to-charge ( $m/z$ ) limit of <4000. Thus, new improved methods of mass-specific tissue imaging, especially at AP, are needed.

From the <sup>‡</sup>Department of Chemistry, Wayne State University, Detroit, Michigan 48202, <sup>§</sup>Gill Center for Biomolecular Science and the Department of Psychological and Brain Sciences, Indiana University, Bloomington, Indiana 47405, and <sup>¶</sup>Department of Chemistry and Biochemistry, University of the Sciences, Philadelphia, Pennsylvania 19104

✂ Author's Choice—Final version full access.

Received, May 13, 2010, and in revised form, September 10, 2010  
Published, MCP Papers in Press, September 20, 2010, DOI 10.1074/mcp.M110.000760

<sup>1</sup> The abbreviations used are: API, atmospheric pressure ionization; LTQ, linear trap quadrupole; ETD, electron transfer dissociation; AP, atmospheric pressure; LSI, laserspray ionization; FWHH, full width at half-height; 2,5-DHAP, 2,5-dihydroxyacetophenone; 2,5-DHB, 2,5-dihydroxybenzoic acid; SA, sinapinic acid.



SCHEME 1. Overview of LSI-MS operated in transmission geometry.

The potential of laserspray ionization (LSI) (Scheme 1) (26–33) for protein tissue analysis is reported here. LSI has advantages relative to other MS-based methods, including speed of analysis, laser ablation of small volumes, more relevant AP conditions, extended mass range and improved fragmentation through multiple charging, and the ability to obtain cross-section data for proteins on appropriate instrumentation. The applicability of LSI for high mass compounds on high performance API mass spectrometers (Orbitrap Exactive and SYNAPT G2) has been demonstrated producing ESI-like multiply protonated ions (26–28). The first experiments showing sequence analysis by ETD using the LSI method were successfully carried out on a Thermo Fisher Scientific (San Jose, CA) LTQ-ETD mass spectrometer (26). Nearly complete sequence coverage was obtained for ubiquitin, an important regulatory protein. Applying ETD fragmentation to LSI-MS analyses potentially provides a new method for studying biological processes, including the mapping of phosphorylation, glycosylation, and ubiquitination sites from intact proteins and directly from tissue.

Furthermore, unlike ESI and related ESI-based methods such as desorption-ESI (34), the LSI method has been shown to allow analysis of lipids in tissue from ablated areas  $<80 \mu\text{m}$  (30). In comparison with literature reports for AP MALDI at the same stage of development (35), LSI is more than an order of magnitude more sensitive and is capable of analyzing proteins on high resolution mass spectrometers as was demonstrated by obtaining full-acquisition mass spectra at 100,000 mass resolution (FWHM,  $m/z$  200) after application of only 20 fmol of bovine pancreas insulin in the matrix 2,5-dihydroxyacetophenone (2,5-DHAP) onto a glass microscope slide (33). The analysis speed of LSI was demonstrated by obtaining mass

spectra of five samples in 8 s (32). Here, we show the utility of LSI for intact peptide and protein analyses directly from mouse brain tissue. The ability to obtain a protein mass spectrum directly from mouse brain tissue in a single laser shot at 100,000 mass resolution and with ETD fragmentation is demonstrated.

#### EXPERIMENTAL PROCEDURES

**Materials**—The matrices 98% 2,5-dihydroxybenzoic acid (2,5-DHB), 99.5% 2,5-DHAP, and 99% sinapinic acid (SA) were purchased from Sigma-Aldrich. The solvents acetonitrile (ACN), trifluoroacetic acid (TFA), and ethanol (EtOH) were purchased from Fisher Scientific Inc. Purified water was used (Millipore, Billerica, MA). The plain microscopy glass slides ( $76.2 \times 25.4 \times 1 \text{ mm}$  in dimensions) were obtained from Gold Seal Products (Portsmouth, NH). Indium-tin oxide-coated conductive glass slides for imaging experiments were a gift from Bruker (Billerica, MA).

**Mouse Brain Tissue**—C57 Bl/6 mice (20 weeks old) were euthanized with  $\text{CO}_2$  gas and transcardially perfused with ice-cold  $1 \times$  phosphate-buffered saline (150 mM NaCl, 100 mM  $\text{NaH}_2\text{PO}_4$ , pH 7.4) for 5 min to remove red blood cells. The brains were frozen at  $-22^\circ\text{C}$  and sliced into  $10\text{-}\mu\text{m}$  sections in sequence using a Leica CM1850 cryostat (Leica Microsystems Inc., Bannockburn, IL). The tissue sections were placed onto prechilled microscopy glass slides (plain or gold-coated) that were briefly warmed with the finger from behind to allow sections to relax and attach. Care was taken to avoid water condensation by storing (at  $-20^\circ\text{C}$ ) and transporting (under dry ice) the tissue-mounted glass slides in an airtight box containing desiccant until use.

**Analysis of Aged and Fresh Tissue Samples**—The mouse brain tissue sections used in this study were shipped in dry ice before being delipidated and then again shipped overnight in dry ice. The aged, delipidated tissue sample was stored for approximately 2 months at  $-5^\circ\text{C}$ . The delipidation was initially obtained on the aged tissue sample and verified by MALDI-time-of-flight (TOF)-MS analysis. The optimized delipidation conditions were used for further study comparing results obtained from MALDI- and LSI-MS analysis.

A second set of mouse brain tissue samples were cut, frozen, and immediately shipped overnight. Each microscopy glass slide, plain and gold-coated, was mounted with four to five tissue sections. On receipt of the frozen samples, delipidation of the tissue on glass slides was performed as described below, and again the samples were immediately frozen and shipped overnight for prompt LSI-MS analysis on an Orbitrap Exactive (Thermo Fisher Scientific) mass spectrometer. These samples were again frozen and shipped overnight for microscopy and subsequent MALDI-MS and LSI LTQ Velos analysis.

**Delipidation of Tissue**—The lipids in the tissue sections were removed according to a published procedure (36). Briefly, the glass slide mounted with tissue was dried in the desiccator before washing twice with ethanol. In the first wash, the glass slide with the mounted tissue was immersed in a glass Petri dish filled with 70% EtOH, swirled for 30 s, and removed carefully. The glass slide was then tilted to remove the solvent for about 10 s and immediately washed with 95% EtOH in another Petri dish for an additional 30 s. After the second wash, the glass slide was allowed to dry in the desiccator for 20 min prior to analysis or stored at approximately  $-20^\circ\text{C}$  until use or shipment under dry ice.

**LSI-MS of Mouse Brain Tissue**—As reported previously (26, 27, 30), LSI on either the Orbitrap Exactive or LTQ Velos mass spectrometer involved removal of the Ion Max source and overriding the interlocks or removing the front and side windows to allow laser and sample access to the ion entrance orifice. Briefly, the laser beam (337 nm;

Newport Corp. VSL-337ND-S) was aligned (180°) with the ion entrance orifice of the mass spectrometer (Scheme 1) and focused using a 120-mm-focal length lens (Orbitrap Exactive) and 102- and 292-mm-focal length lenses from CVI Melles Griot, Albuquerque, NM for the Thermo Fisher Scientific LTQ Velos instrument. The glass microscope slide mounted with mouse brain tissue was prepared with the LSI matrix (2,5-DHB, 5 mg ml<sup>-1</sup>; or 2,5-DHAP, saturated solution) dissolved in 50:50 ACN:water by placing a number of 0.2- $\mu$ l drops on top of the tissue material and allowing them to air dry. After solvent evaporation, the glass slide containing LSI matrix applied to mouse brain tissue was placed 2–3 mm in front of the mass spectrometer ion transfer tube entrance and was moved manually through the laser beam, which was aligned 180° relative to the ion entrance orifice (transmission geometry). The AP to vacuum ion transfer capillary was heated to 375 °C for 2,5-DHB and 300 °C for 2,5-DHAP, and the laser fluence per pulse was about 0.5–1 J cm<sup>-2</sup>. Multiply charged ions were observed in the absence of an electric field in the ion source region. Both plain and gold-coated glass slides were used.

**High Resolution Orbitrap Instrument**—Positive ion mass spectral acquisition was set for 1 s giving 100,000 mass resolution, and the maximum injection time was set at 100 ms. The laser was fired at ~4–6 Hz during acquisition while the tissue covered with matrix above or below the tissue using solvent-based or solvent-free procedures (14, 30) was constantly moved through the laser beam except for experiments in which mass spectra from single laser shots were acquired by firing the laser at less than 1 Hz.

**LTQ-ETD Instrument**—LSI-MS and -MS/MS were performed on an LTQ Velos instrument with ETD capabilities. Full MS was obtained in positive ion mode for 1 min. A mixture of ultrapure helium and nitrogen (25% helium and 75% nitrogen; purity, >99.995%) was used as the reaction gas to perform the ETD experiments. The reaction time was set at 120 ms using an isolation width of 3 amu. The activation time ranged from 25 to 50 ms for the precursor ions 917.5 (2+), 1491 (12+), and 1789 (10+). A supplemental activation of 20 V was used for the 2+ precursor ion. A single 0.33-s acquisition was selected to obtain the ETD fragment ion mass spectra for peptide identification; the total ETD acquisition time was set for 1 min.

**LSI Tissue Imaging**—Mouse brain tissue mounted on a glass microscope slide and coated with a saturated solution of 2,5-DHAP in 1:1 ACN/H<sub>2</sub>O using 0.2- $\mu$ l drops was controllably moved through the laser beam with ablation in transmission geometry, as described above, using an eTrack series xy-stage (Newmark Systems, Mission Viejo, CA). Lanes were at 100- $\mu$ m intervals, and each lane was 10 mm long from which 22 s of data were acquired. For these studies, three mass spectral acquisitions were obtained per second with the laser operating at ~12 Hz. The ablated diameter for each laser shot was ~15  $\mu$ m (neglecting the stray beam commonly observed), which converts to an area of about 4(15)  $\times$  15  $\mu$ m<sup>2</sup> ablated per MS acquisition.

**MALDI-MS of Mouse Brain Tissue**—A MALDI-TOF Bruker Ultraflex mass spectrometer (Bruker, Bremen, Germany) equipped with a nitrogen laser (337 nm) was used to monitor the success of the tissue delipidation and for comparison with LSI results. The MALDI sample preparation was performed according to published work (36). After washing the tissue and drying in the desiccator, the tissue was spotted with 0.2  $\mu$ l of either SA matrix dissolved in 50:50 ACN:water in 0.1% TFA or 2,5-DHAP in 50:50 ACN:water. The mass spectrum was acquired using the linear positive ion mode with an accelerating voltage of 20.16 kV, extraction voltage of 18.48 kV, lens voltage of 7.06 kV, and pulsed ion extraction of 360 ns. Delayed extraction parameters were optimized to have the optimal resolution and sensitivity for the MALDI range was 12-kDa. An increment of 30 laser shots was used, and shots were positioned and moved within a single matrix spot to obtain a mass spectrum having a total of 120 laser

shots. The mass spectrum was processed and base line-corrected using the Flex Analysis software. Both plain and gold-coated microscopy slides were used; only gold-coated microscopy slides are expected to provide the correct mass calibration.

**Data Analysis**—MASCOT Distiller version 2.3.2.0 (Matrix Science, London, UK) (37) was used to interpret ETD mass spectra for peptide and protein identification obtained from the LTQ-ETD Velos. The Mass Spectrometry protein sequence DataBase (MSDB) was searched using the no enzyme setting to obtain the sequence analyses directly from mouse tissue. Parameters were set to include acetylation, deamination, oxidation, methylation, and phosphorylation. The peptide and protein masses had to be within the mass tolerance characteristic of the mass spectrometer used for data acquisition. Searches within 1-Da mass error were performed, but to consider a peptide as well matched, it had to be within <5 ppm of the mass obtained from the Orbitrap Exactive.

**Microscopy Measurement**—Optical microscopy (Nikon Eclipse LV100) was performed to obtain qualitative information on the spatial area of matrix/tissue ablated per laser shot after mass spectral analysis of the tissue using LSI. Various magnification conditions were used, ranging from 5 $\times$  to 100 $\times$ , providing detailed views to ~1- $\mu$ m resolution. Microscopy data were obtained for both the aged and fresh tissue samples from which mass spectra were acquired on both the LTQ Velos and the Orbitrap Exactive mass spectrometers.

## RESULTS AND DISCUSSIONS

**Evaluation of Experimental Conditions on Aged Tissue Sample**—Tissue fixation or washing with solvents to extract lipids enhances the signal quality of peptides and proteins and slows enzymatic processes, thus extending the useful life prior to analysis (38). The washing solvent was selected based on previously reported studies (36, 39) as well as from results we obtained from MALDI-MS analyses of tissue extracted with recommended solvents, ethanol and isopropanol. Here, the ethanol wash was selected because it gave higher intensity protein MALDI-MS signals using SA as the matrix. The guidelines developed by Schwartz *et al.* (40) for the proper handling of tissue sections (tissue storage, sectioning, and mounting) for peptide and protein analyses were applied. The choice of matrix and its deposition onto the tissue have been shown to be important in determining the subset of proteins extracted from the tissue and detected using MALDI (39). For the MALDI analysis of the delipidated mouse brain tissue, peptide and protein signals were detected using SA as matrix from *m/z* 5000 to 19,000 (supplemental Fig. S1), which is within the range that Seeley *et al.* (36) presented; the mass calibration is expected to be somewhat off for results in which plain microscopy glass slides without conductive coating were used. Only a few of the proteins detected give significant signal intensity similar to previous studies (12).

Once a satisfactory procedure for handling and delipidating mouse brain tissue was established for MALDI analysis, that method was applied for LSI-MS. Using 2,5-DHB as matrix, only lipids were observed even with the delipidated tissue, similar to a previous report (30). However, for the delipidated tissue using 2,5-DHAP, lipids were observed in low abundance if at all, and signals for multiply charged ions having masses as high as 5–19 kDa (at ZS1) were detected. A mass

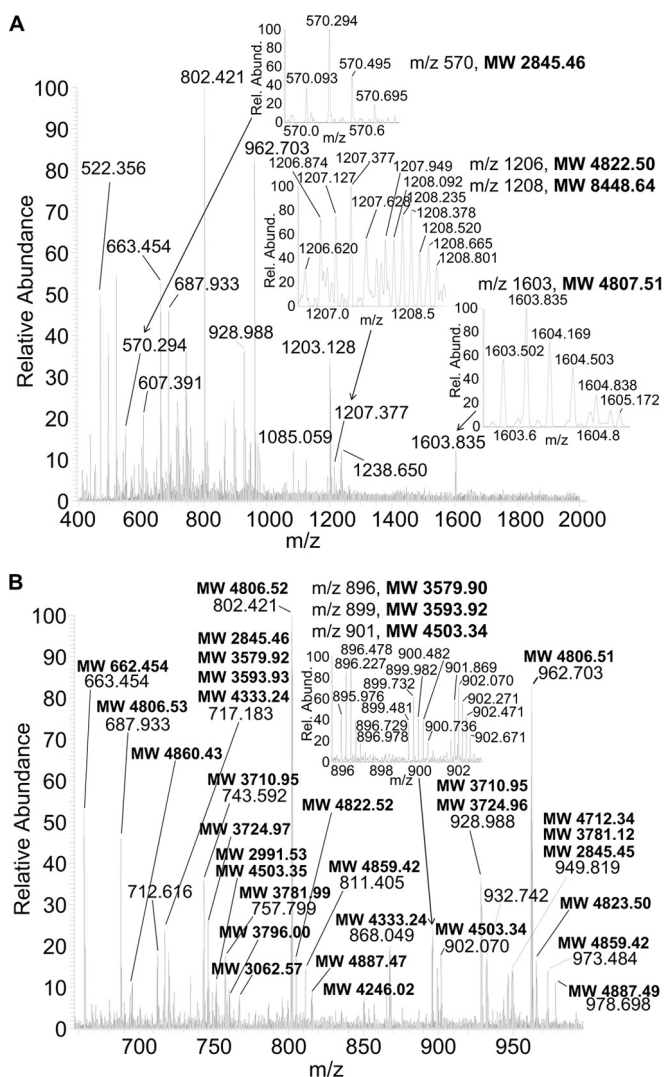


**FIG. 1.** LSI mass spectra from aged mouse brain tissue washed with ethanol and spotted with 2,5-DHAP matrix in 50:50 ACN: water using an Orbitrap Exactive mass spectrometer. **A**, full mass spectrum with insets showing multiple charged protein and peptide ions. **B**, limited mass range between  $m/z$  650 and 1000 is displayed with monoisotopic molecular weights of the various multiply charged ions presented. *Rel. Abund.*, relative abundance.

spectrum obtained from the Orbitrap Exactive at 100,000 (FWHM,  $m/z$  200) mass resolution by summing 15 1-s acquisitions is shown in Fig. 1 and represents ablation of most of the tissue covered by a 0.2- $\mu$ l solution of 2,5-DHAP. Because the mass resolution of the Orbitrap Exactive provides  $^{13}\text{C}$  isotope separation even for proteins, a single  $^{13}\text{C}$  isotope distribution is all that is necessary to determine the monoisotopic protein molecular weight with high mass accuracy (Fig. 1, insets). Ions observed just above noise, for which the monoisotopic peak cannot be reliably identified, provide a more accurate average mass than obtained with linear MALDI-TOF instruments. Fig. 1B is the inset region from Fig. 1A with the mass range displayed between  $m/z$  650 and 1000.

The multiply charged ions range from 3+ to 8+, representing ions having molecular masses from approximately 650 to 5000 Da. For this data set, most ions were from compounds below 10 kDa. Because of the long storage time for the aged sample, it is possible that some of the observed multiply charged ions are from post-mortem enzymatic digestion of proteins (12, 36). The use of gold-coated and plain microscopy glass slides provides comparable abundance LSI mass spectra of the delipified tissue. As expected, no mass shift was observed in the AP LSI results using conductive or non-conductive glass slides; matrix placed below the tissue increased the ion abundance at the expense of a larger ablated area. Experiments without the addition of the LSI matrix did not provide any useful analytical results.

Microscopy images of the aged mouse brain tissue after LSI analysis showed a variety of ablated areas, including numerous areas where the laser beam did not appear to penetrate the tissue (supplemental Fig. S2). The areas in which the tissue was completely ablated ranged in dimensions from  $\sim 3$  to  $9 \mu\text{m} \times \sim 5$  to  $25 \mu\text{m}$ . Because the laser was fired at several hertz as the tissue was constantly moved through the laser beam, each 1-s acquisition was the sum of several laser shots. The elongated features observed in the microscopy image may be the result of multiple laser shots producing continuous ablation as the tissue was moved slowly through the beam. Holes in the tissue that appear to be from a single laser shot were typically  $< 30 \mu\text{m}^2$  (supplemental Fig. S3). For the 10- $\mu\text{m}$  tissue thickness used in this study, these microscopy data suggest that the tissue volume below the ablated area represents  $\sim 300 \mu\text{m}^3$  for a single laser shot. However, to achieve this spatial resolution will minimally require matrix preparation methods that result in no diffusion of compounds outside the boundary area and improved mass spectral sensitivity.

**Comparison of LSI-MS and MALDI-MS Analysis on Fresh Tissue Samples**—Successful results with the aged tissue samples prompted us to examine fresh tissue sections that were maintained at or below  $-20^\circ\text{C}$  except for short times required for mounting the tissue to the glass slide, delipification, mass spectral analysis, and microscopy. The fresh delipified samples using 2,5-DHAP matrix and acquired on the Orbitrap Exactive showed an abundant doubly charged LSI ion at  $m/z$  917.50 (molecular weight 1833.0) and numerous other multiply charged ions at higher  $m/z$  values (Fig. 2). The highest mass protein with at least two observed charge state distributions had a molecular mass (monoisotopic) of 17,882 Da, although a single low abundance isotope distribution was observed for an ion having an average molecular mass of  $\sim 19,665$  Da. Some of the lower molecular weight proteins observed in the aged tissue sample (Fig. 1) were also observed in the fresh sample but in lower abundance, whereas the higher mass proteins were significantly more abundant in the fresh tissue sample. Supplemental Fig. S4 shows that in a single laser shot the most abundant proteins were observed

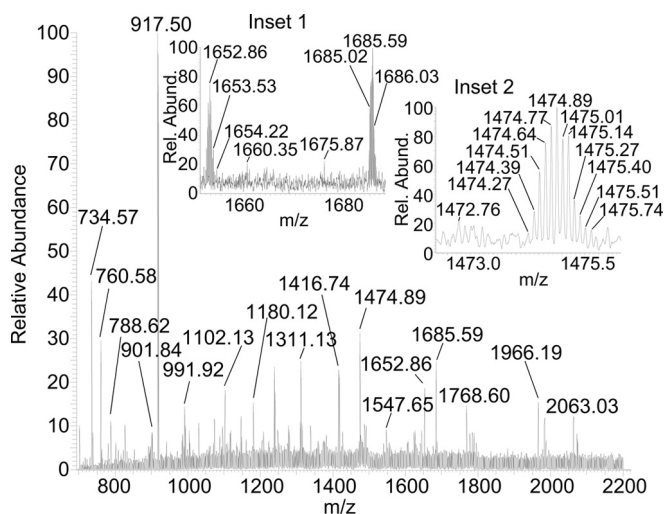


FIG. 2. LSI-MS summed full and *inset* mass spectra of delipified fresh tissue on plain glass slide spotted with 2,5-DHAP matrix in 50:50 ACN:water showing multiple charged protein ions using Orbitrap Exactive mass spectrometer. *Rel. Abund.*, relative abundance.

from the fresh tissue using the 100,000 mass resolution setting of the Orbitrap Exactive. The mass spectra for the single laser shot, the sum of seven laser shots, and the sum of the full acquisition for a 0.2- $\mu$ l matrix deposition are shown in supplemental Fig. S4B. Notable differences between gold-coated (supplemental Fig. S4) and plain glass slides (Fig. 2) were again not observed. Supplemental Fig. S5 shows three isotope distributions each for multiply charge ions representing proteins having molecular masses of 9908, 11,788, and 12,369 Da (monoisotopic mass).

A fresh tissue section from the same mouse was delipified and immediately mass-measured on an LTQ Velos instrument. The multiply charged ions described above for fresh tissue were observed. The mass spectrum from summing multiple acquisitions on the tissue slice is provided in Fig. 3A. The distribution of multiple charged ions of the protein having molecular weight 11,788, however, could be observed in a single acquisition representing one laser shot (Fig. 3B1). Single laser shots in different areas of the mouse brain tissue gave different results. For example, Fig. 3B2, also from a single laser shot, shows the protein at molecular weight 17,882 in lower abundance than the first protein of molecular weight 11,788, and a peptide having a molecular weight of 1833 was observed more in the center than the edges of the tissue. The ability to acquire a mass spectrum from a single laser shot using a relatively inexpensive nitrogen laser suggests the potential for high speed tissue imaging.

**Potential of Tissue Imaging Using LSI**—To evaluate the potential for tissue imaging using LSI, a crude experiment was performed using a glass slide with mounted mouse brain tissue that was coated with the matrix 2,5-DHAP by depositing 0.2- $\mu$ l droplets of a saturated solution of 1:1 ACN:H<sub>2</sub>O over the tissue surface and allowed to air dry. This matrix

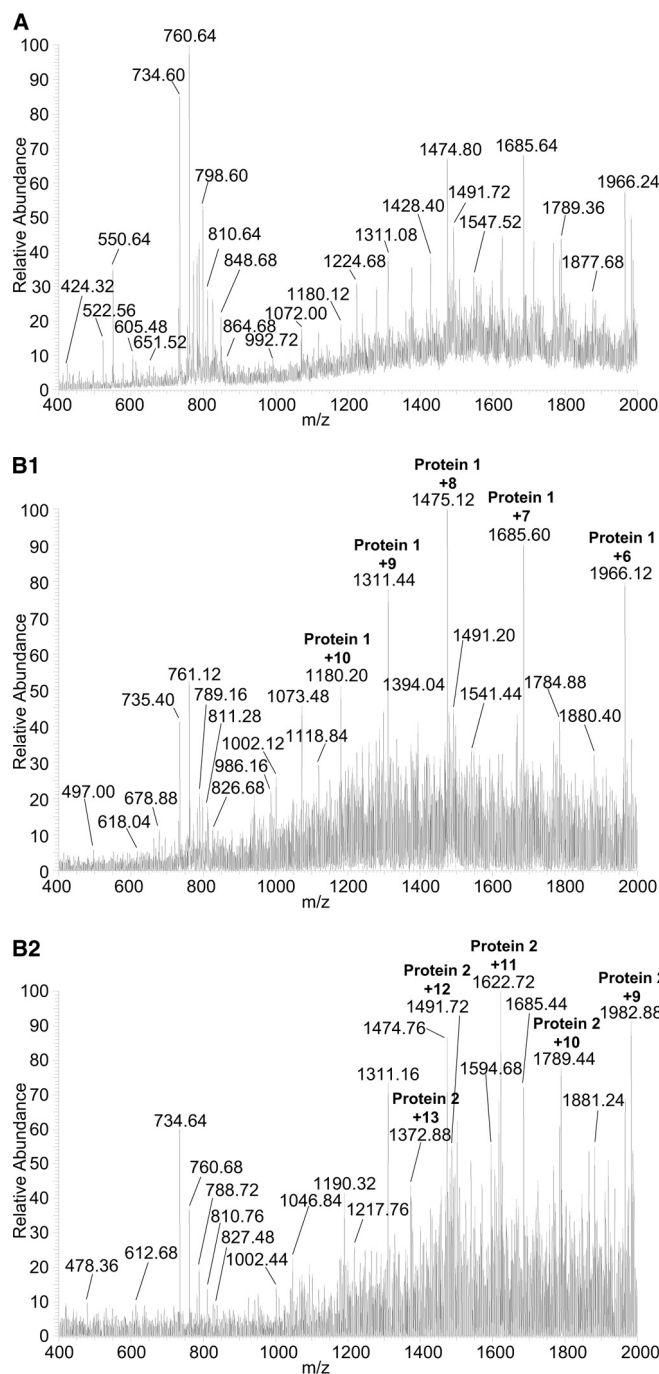


FIG. 3. LSI-MS spectra of delipified fresh tissue on plain glass slide spotted with 2,5-DHAP matrix in 50:50 ACN:water using LTQ Velos. A, sum of the full acquisition. B1 and B2, single acquisitions at different tissue locations showing different protein abundances. The ions observed around *m/z* 760 are from lipids.

deposition method is not suitable for tissue imaging because delocalization of compounds in the tissue and uneven matrix deposition are expected with this approach. An attempt at spray applying the matrix from solution, which is a more appropriate matrix deposition method, resulted in very low abundances of peptide and protein ions (supplemen-

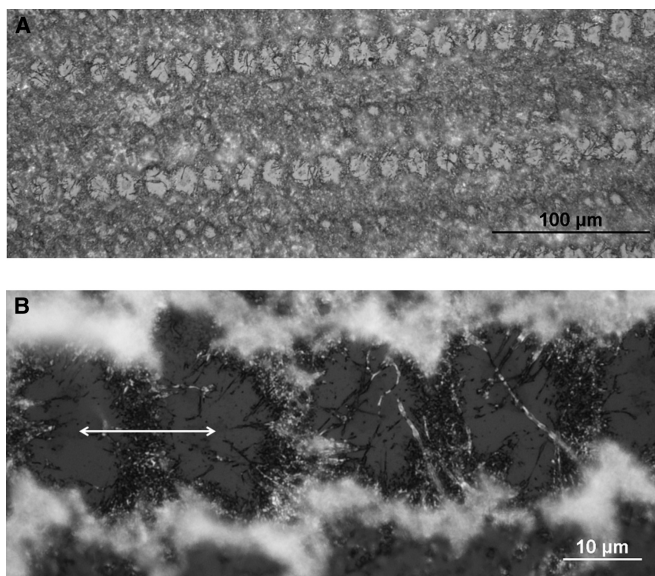


FIG. 4. **Optical images of laser-ablated areas obtained in imaging experiment.** A, 20 $\times$  magnification. B, 100 $\times$  magnification. Arrow denotes 15  $\mu\text{m}$ .

tal Fig. S6). Clearly, improved matrix preparation conditions for LSI imaging are needed. Nevertheless, attaching the glass microscope slide to a computer controlled xy-stage allowed a crude image of mouse brain tissue to be obtained. Mass-specific imaging for two charge states of the protein with molecular weight 11,788 and one charge state of the protein with molecular weight 12,369 is shown in [supplemental Fig. S7](#). Several other peptides and proteins gave sufficient signal intensities in single acquisitions to produce crude images. Obtaining higher shot-to-shot reproducibility and increased analyte ion abundances are areas that require further research.

Microscopy images of the laser-ablated tissue after the imaging analysis are shown in Fig. 4. Rows spaced at 100- $\mu\text{m}$  intervals of single laser shots are readily seen. The individual laser-ablated areas in this experiment, as determined by optical microscopy, are  $\sim 15 \mu\text{m}$  in diameter. The mass spectrum shown in [supplemental Fig. S8](#) is of a single MS acquisition during which time four laser shots impacted the tissue in adjacent positions. Thus, each mass spectral acquisition was of a visibly ablated area of approximately  $15 \times 4 \times 15 \mu\text{m}^2$ . It is clear from these images that the laser beam frequently completely ablates the tissue and matrix producing sufficient ions to be detected. The 10- $\mu\text{m}$ -thick tissue slices likely absorb a fraction of the laser energy before it is absorbed by the matrix.

The LSI method introduces remarkable speed and simplicity of analysis compared with reflective geometry MALDI where frequently  $>100$  laser shots are summed to provide each data point in the image (41, 42). For tissue imaging experiments, high repetition and therefore expensive lasers are required to keep the analysis time reasonable (hours ver-

sus days). The ability to obtain mass spectra of proteins directly from tissue in a single or even a few summed laser shots using the LSI approach suggests the potential for using less expensive lasers to achieve comparable analysis speed relative to high repetition laser MALDI. For the crude imaging experiment reported here, the laser repetition rate was  $\sim 12$  Hz, and each lane received 89 laser shots in 22 s. With 100- $\mu\text{m}$  spacing between rows, 80 rows were required to image the mouse brain tissue. Thus, actual acquisition time was only about 30 min. This work demonstrates the potential speed of this method for tissue analysis or imaging.

The ability to obtain mass spectra of proteins directly from tissue using LSI offers considerable potential in tissue analysis. However, difficulties that need to be addressed before tissue imaging becomes a reality using LSI are increased ion abundances from single acquisitions and higher shot-to-shot reproducibility. We expect reproducibility is related to uneven tissue thickness, the condition of the tissue, matrix application, and the laser flux per unit area. Just as in MALDI imaging, matrix application in LSI is a crucial step. The dried droplet method of spotting matrix that was used in the present study is inappropriate for tissue imaging studies. We are currently beginning research aimed at improving solvent-based and solvent-free matrix preparation methods for tissue imaging using LSI. Future advances also need to incorporate solvent-free gas-phase separation for efficient simplification of complexity of the produced gas-phase ions (28, 29, 43).

For comparison purposes, sequential tissue sections from the same mouse brain used for the fresh tissue studies mounted on gold-coated and plain glass slides were used for vacuum MALDI-MS analysis. One-half of each delipidified tissue section was coated with 2,5-DHAP, and the other half was coated with SA applying several 0.2- $\mu\text{l}$  matrix solutions. Interestingly, none of the observed molecular weights are common between LSI using 2,5-DHAP and MALDI using either 2,5-DHAP or SA. MALDI with the 2,5-DHAP matrix gave poor results, which may help explain the different proteins observed between vacuum MALDI and LSI.

**ETD Fragmentation of Peptides Directly from Tissue**—Because LSI produces ESI-like multiply charged mass spectra directly from tissue, it becomes possible to achieve ETD fragmentation of these ions. This is demonstrated for the doubly charged peptide ion that was observed at  $m/z$  917.5 (molecular weight 1833) for a single ETD acquisition representing four single laser shots, each on fresh spots of the tissue obtained on the LTQ-ETD Velos mass spectrometer (Fig. 5). Table I shows the result of the MASCOT search obtained from the single acquisition data. A MASCOT score of 73 (67 is considered to be significant) was achieved for the peptide having the sequence Ac-ASQKRPSQRSKYLATA that also is well within the 5-ppm mass tolerance for this peptide acquired on the Orbitrap Exactive. This sequence encodes for the myelin basic protein N-terminal fragment that is known to occur in mouse brain. The labeled masses in Fig. 5 are the

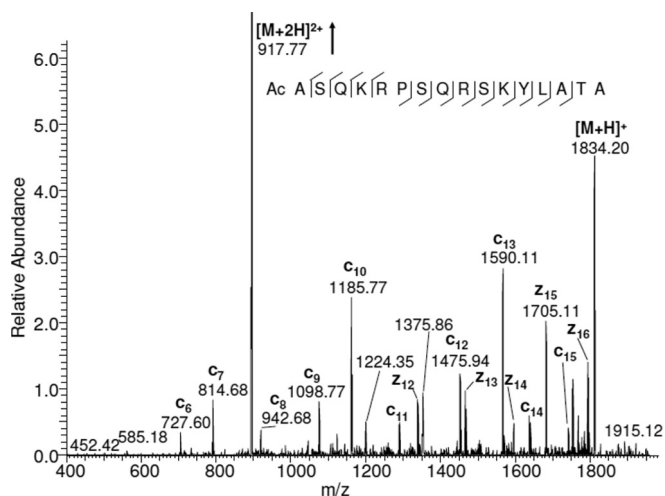


FIG. 5. LSI-ETD single scan acquisition mass spectrum at precursor ion 917.5 (2+) of delipified fresh tissue on plain glass slide spotted with 2,5-DHAP matrix in 50:50 ACN:water using LTO Velos.

TABLE I  
LSI-ETD MASCOT scores for  $m/z$  917.5

The Delta value is the difference between the calculated mass for the sequence shown and the accurate mass measurement obtained from the Orbitrap at 100,000 mass resolution. Only sequences with a Delta < 0.005 were within the mass tolerance of the mass.

Score	$M_r$ (calculated)	Delta	Sequence
73.1	1832.9856	-0.0002	ASQKRPSQRSKYLATA
65.1	1832.9856	-0.0002	ASQKRPSQRSKYLATA
41.0	1832.7539	0.2315	ADLTSCSSLKKEEVYH
41.0	1832.7539	0.2315	ADLTSCSSLKKEEVYH
40.5	1832.8686	0.1168	ADEMKEIQERQRDK
40.5	1832.6936	0.2918	SVLYQYQTHSKR
40.3	1832.8370	0.1485	AEWIFGGVKYQYGGNQ
40.3	1832.8791	0.1063	ANIYKNKKSHEQLSA
40.2	1832.9631	0.0223	ANLKYNQLEKKNNA
40.2	1832.9631	0.0223	ANLKYNQLEKKNNA

predicted "c" and "z" fragments expected from ETD fragmentation of this peptide. The only missing sequence ions are related to the proline residue. It is clear that synergy exists between accurate mass measurement and ETD for reducing the number of hits obtained by database searching. ETD fragment ions and accurate mass measurement were also obtained for  $m/z$  1491 and  $m/z$  1789, which are the 12+ and 10+ charge states, respectively, for the protein of molecular weight 17,889 (supplemental Fig. S9). We are in the process of attempting to identify this protein; MASCOT interpretation searches currently only permit charge states up to 8+. These first results demonstrate the potential of LSI for protein identification directly from tissue and are a significant advance over current methods in which the identity of the ions observed are made only from an approximate average mass value of the proteins known to be in the tissue.

**Conclusion**—The first example of peptides and proteins observed directly from tissue producing multiply charged ions

is reported. The ability to use high performance API mass spectrometers for analyses provides isotopic resolution and accurate mass measurement even for proteins (44). The multiply charged ions are demonstrated to allow ETD fragmentation of ions desorbed directly from tissue for improved compound identification (45). Myelin basic protein N-terminal fragment peptide was identified from a single ETD acquisition directly from tissue. Fragmentation by advanced techniques such as ETD is not applicable using MALDI tissue imaging because of the low charge states of the ions produced. The time-of-flight mass analyzers used in vacuum MALDI, although providing mass resolution in excess of 10,000 and mass accuracies better than 20 ppm (3), are less available than API mass spectrometers and are inadequate for directly identifying or even confirming a protein structure from tissue. Initial studies aimed toward tissue imaging at AP using LSI are encouraging because of the ability to ablate small areas and to obtain multiply charged mass spectra of proteins even from a single laser shot. With the LSI approach, the advantages of MALDI in achieving reduced ablated areas from solid samples and the advantages of ESI for extending the mass range of high performance instruments to allow high mass resolution and accurate mass analysis as well as advanced fragmentation are demonstrated.

**Acknowledgments**—We are grateful to Professor J. Michael Walker (Indiana University) for the motivation. Andrew Harron (University of the Sciences) is gratefully acknowledged for processing the mouse brain images.

\* This work was supported, in whole or in part, by National Institutes of Health Grant DA021696 (to K. M.). This work was also supported by Wayne State University through a Rumble fellowship (to E. D. I.), a summer research award (to A. L. R.), and start-up funds (to S. T.); National Science Foundation Faculty Early Career Development (CAREER) Grant 0955975 (to S. T.); an American Society for Mass Spectrometry Research Award financially supported by Waters Co. (to S. T.); a DuPont Co. Young Investigator Research Award (to S. T.); and the University of the Sciences through a Richard E. Hough-ton endowment (to C. N. M.).

§ This article contains supplemental Figs. S1–S9.

|| To whom correspondence should be addressed: Dept. of Chemistry, Wayne State University, 5101 Cass Ave., Detroit, MI 48202. Tel.: 313-577-9823; E-mail: strimpin@chem.wayne.edu.

## REFERENCES

- Fournier, I., Wisztorski, M., and Salzet, M. (2008) Tissue imaging using MALDI-MS: a new frontier of histopathology proteomics. *Expert Rev. Proteomics* **5**, 413–424
- Bedair, M., and Sumner, L. W. (2008) Current and emerging mass-spectrometry technologies for metabolomics. *Trends Anal. Chem.* **27**, 238–250
- McDonnell, L. A., and Heeren, R. M. (2007) Imaging mass spectrometry. *Mass Spectrom. Rev.* **26**, 606–643
- Jackson, S. N., Ugarov, M., Egan, T., Post, J. D., Langlais, D., Schultz, J. A., and Woods, A. S. (2007) MALDI-ion mobility-TOFMS imaging of lipids in rat brain tissue. *J. Mass Spectrom.* **42**, 1093–1098
- Khatib-Shahidi, S., Andersson, M., Herman, J. L., Gillespie, T. A., and Caprioli, R. M. (2006) Direct molecular analysis of whole-body animal tissue sections by imaging MALDI mass spectrometry. *Anal. Chem.* **78**, 6448–6456

6. Chaurand, P., Cornett, D. S., and Caprioli, R. M. (2006) Molecular imaging of thin mammalian tissue sections by mass spectrometry. *Curr. Opin. Biotechnol.* **17**, 431–436
7. Chaurand, P., Schwartz, S. A., and Caprioli, R. M. (2002) Imaging mass spectrometry: a new tool to investigate the spatial organization of peptides and proteins in mammalian tissue sections. *Curr. Opin. Chem. Biol.* **6**, 676–681
8. Stoeckli, M., Chaurand, P., Hallahan, D. E., and Caprioli, R. M. (2001) Imaging mass spectrometry: a new technology for the analysis of protein expression in mammalian tissues. *Nat. Med.* **7**, 493–496
9. Ostrowski, S. G., Van Bell, C. T., Winograd, N., and Ewing, A. G. (2004) Mass spectrometric imaging of highly curved membranes during *Tetrahymena* mating. *Science* **305**, 71–73
10. Winograd, N. (2005) The magic of cluster SIMS. *Anal. Chem.* **77**, 142A–149A
11. Jones, E. A., Lockyer, N. P., and Vickerman, J. C. (2008) Depth profiling brain tissue sections with a 40 keV C-60(+) primary ion beam. *Anal. Chem.* **80**, 2125–2132
12. Chaurand, P., Schwartz, S. A., and Caprioli, R. M. (2004) Assessing protein patterns in disease using imaging mass spectrometry. *J. Proteome Res.* **3**, 245–252
13. Zimmerman, T. A., Monroe, E. B., and Sweedler, J. V. (2008) Adapting the stretched sample method from tissue profiling to imaging. *Proteomics* **8**, 3809–3815
14. Trimpin, S., Herath, T. N., Inutan, E. D., Wager-Miller, J., Kowalski, P., Claude, E., Walker, J. M., and Mackie, K. (2010) Automated solvent-free matrix deposition for tissue imaging by mass spectrometry. *Anal. Chem.* **82**, 359–367
15. Deininger, S. O., Suckau, D., Becker, M., and Schuerenberg, M. (2009) MALDI-tissue imaging at high resolution and speed: essential steps towards its applications in histology, in *Proceedings of the 57th ASMS Conference on Mass Spectrometry and Allied Topics, Philadelphia, May 31–June 4, 2009*, American Society for Mass Spectrometry, Santa Fe, NM
16. Pierson, J., Norris, J. L., Aerni, H. R., Svenningsson, P., Caprioli, R. M., and Andr en, P. E. (2004) Molecular profiling of experimental Parkinson's disease: direct analysis of peptides and proteins on brain tissue sections by MALDI mass spectrometry. *J. Proteome Res.* **3**, 289–295
17. Rohner, T. C., Staab, D., and Stoeckli, M. (2005) MALDI mass spectrometric imaging biological tissue sections. *Mech. Ageing Dev.* **126**, 177–185
18. Touboul, D., Piedno el, H., Voisin, V., De La Porte, S., Brunelle, A., Halgand, F., and Lapr evote, O. (2004) Changes in phospholipid composition within the dystrophic muscle by matrix-assisted laser desorption/ionization mass spectrometry and mass spectrometry imaging. *Eur. J. Mass Spectrom.* **10**, 657–664
19. Chaurand, P., Schwartz, S. A., and Caprioli, R. M. (2004) Profiling and imaging proteins in tissue sections by MS. *Anal. Chem.* **76**, 86A–93A
20. Syka, J. E., Coon, J. J., Schroeder, M. J., Shabanowitz, J., and Hunt, D. F. (2004) Peptide and protein sequence analysis by electron transfer dissociation mass spectrometry. *Proc. Natl. Acad. Sci.* **101**, 9528–9533
21. Mikesh, L. M., Ueberheide, B., Chi, A., Coon, J. J., Syka, J. E., Shabanowitz, J., and Hunt, D. F. (2006) The utility of ETD mass spectrometry in proteomic analysis. *Biochim. Biophys. Acta* **1764**, 1811–1822
22. Han, H., Xia, Y., Yang, M., and McLuckey, S. A. (2008) Rapidly alternating transmission mode electron-transfer dissociation and collisional activation for the characterization of polypeptide ions. *Anal. Chem.* **80**, 3492–3497
23. Landgraf, R. R., Prieto Conaway, M. C., Garrett, T. J., Stacpoole, P. W., and Yost, R. A. (2009) Imaging of lipids in spinal cord using intermediate pressure matrix-assisted laser desorption-linear ion trap/Orbitrap MS. *Anal. Chem.* **81**, 8488–8495
24. Tanaka, K., Waki, H., Ido, Y., Akita, S., Yoshida, Y., and Yoshida, T. (1988) Protein and polymer analyses up to m/z 100 000 by laser ionization time-of-flight mass spectrometry. *Rapid Commun. Mass Spectrom.* **2**, 151–153
25. Karas, M., and Hillenkamp, F. (1988) Laser desorption ionization of proteins with molecular masses exceeding 10 000 Daltons. *Anal. Chem.* **60**, 2299–2301
26. Trimpin, S., Inutan, E. D., Herath, T. N., and McEwen, C. N. (2010) Laserspray ionization: a new AP-MALDI method for producing highly charged gas-phase ions of peptides and proteins directly from solid solutions. *Mol. Cell. Proteomics* **9**, 362–367
27. Trimpin, S., Inutan, E. D., Herath, T. N., and McEwen, C. N. (2010) A matrix-assisted laser desorption/ionization mass spectrometry method for selectively producing either singly or multiply charged molecular ions. *Anal. Chem.* **82**, 11–15
28. Inutan, E., and Trimpin, S. (2010) Laserspray ionization (LSI) ion mobility spectrometry (IMS) mass spectrometry (MS). *J. Am. Soc. Mass Spectrom.* **21**, 1260–1264
29. Trimpin, S. (2010) A perspective on MALDI alternatives—total solvent-free analysis and electron transfer dissociation of highly charged ions by laserspray ionization. *J. Mass Spectrom.* **45**, 471–485
30. Trimpin, S., Herath, T. N., Inutan, E. D., Cernat, S. A., Miller, J. B., Mackie, K., and Walker, J. M. (2009) Field-free transmission geometry atmospheric pressure matrix-assisted laser desorption/ionization for rapid analysis of unadulterated tissue samples. *Rapid Commun. Mass Spectrom.* **23**, 3023–3027
31. McEwen, C. N., Larsen, B. S., and Trimpin, S. (2010) Selecting singly or multiply charged ions using a commercial AP-MALDI mass spectrometer ion source. *Anal. Chem.* **82**, 4998–5001
32. Zydell, F., Trimpin, S., and McEwen, C. N. (2010) Laserspray ionization using an atmospheric solids analysis probe for sample introduction. *J. Am. Soc. Mass Spectrom.* **21**, 1889–1892
33. McEwen, C. N., and Trimpin, S. (2010) An alternative paradigm in mass spectrometry? Flying elephants and Trojan horses. *Int. J. Mass Spectrom.*, doi: 10.1016/j.ijms.2010.05.020
34. Tak ats, Z., Wiseman, J. M., Gologan, B., and Cooks, R. G. (2004) Mass spectrometry sampling under ambient conditions with desorption electrospray ionization. *Science* **306**, 471–473
35. Laiko, V. V., Moyer, S. C., and Cotter, R. J. (2000) Atmospheric pressure MALDI/ion trap mass spectrometry. *Anal. Chem.* **72**, 5239–5243
36. Seeley, E. H., Oppenheimer, S. R., Mi, D., Chaurand, P., and Caprioli, R. M. (2008) Enhancement of protein sensitivity for MALDI imaging mass spectrometry after chemical treatment of tissue sections. *J. Am. Soc. Mass Spectrom.* **19**, 1069–1077
37. Perkins, D. N., Pappin, D. J., Creasy, D. M., and Cottrell, J. S. (1999) Probability-based protein identification by searching sequence databases using mass spectrometry data. *Electrophoresis* **20**, 3551–3567
38. Chaurand, P., Norris, J. L., Cornett, D. S., Mobley, J. A., and Caprioli, R. M. (2006) New developments in profiling and imaging of proteins from tissue sections by MALDI mass spectrometry. *J. Proteome Res.* **5**, 2889–2900
39. Kaleta, B. K., van der Wiel, I. M., Stauber, J., G uzel, C., Kros, J. M., Luiders, T. M., and Heeren, R. M. (2009) Sample preparation issues for tissue imaging by imaging MS. *Proteomics* **9**, 2622–2633
40. Schwartz, S. A., Reyzer, M. L., and Caprioli, R. M. (2003) Direct tissue analysis using matrix-assisted laser desorption/ionization mass spectrometry: practical aspects of sample preparation. *J. Mass Spectrom.* **38**, 699–708
41. Chaurand, P., Schriver, K. E., and Caprioli, R. M. (2007) Instrument design and characterization for high resolution MALDI-MS imaging of tissue sections. *J. Mass Spectrom.* **42**, 476–489
42. Caldwell, R. L., and Caprioli, R. M. (2005) Tissue profiling by mass spectrometry: a review of methodology and applications. *Mol. Cell. Proteomics* **4**, 394–401
43. Trimpin, S., and Brizzard, B. (2009) Analysis of insoluble proteins. *Bio-Techniques* **46**, 409–419
44. He, F., Emmett, M. R., H akansson, K., Hendrickson, C. L., and Marshall, A. G. (2004) Theoretical and experimental prospects for protein identification based solely on accurate mass measurement. *J. Proteome Res.* **3**, 61–67
45. Cooper, H. J., H akansson, K., and Marshall, A. G. (2005) The role of electron capture dissociation in biomolecular analysis. *Mass Spectrom. Rev.* **24**, 201–222